Pure & Appl. Chem., Vol.54, No.2, pp.395-406, 1982.
Printed in Great Britain.

0033-4545/82/020395-12$03.00/0
Pergamon Press Ltd

ELECTRO-OPTICAL METHODS FOR CHARACTERISATION OF POLYMERS AND BIOPOLYMERS

B. R. Jennings

Electro-Optics Group, Physics Department, Brunel University, Uxbridge, U.K.

Abstract - When subjected to an electric field, solute molecules partially align. Such alignment is accompanied by a change in one or more of the optical properties of the solution. A brief account is given of the principles, apparatus and utility of various electro-optical phenomena in the realm of polymer science. Examples are given which illustrate the potential of the methods for determining the size, shape, dipole moments and optical characteristics of polymers and biopolymers in solution.

INTRODUCTION

The optical characteristics of polymers have long been recognised as an experimental access to information on their structure (Ref. 1). At the molecular level the majority of molecules are anisotropic in their geometrical, electrical and optical characteristics. In dilute solution, such molecules adopt a random orientational array and the solution as a whole is isotropic. Application of any applied force field, of which an electric field is a particular example, results in the imposition of molecular order. Any inherent anisotropy in the molecular structure is then increasingly evident in the medium as a whole. The induced order can result from either or both the orientation of rigid molecules or the deformation of flexible systems. By passing a beam of light through a solution under such conditions one can monitor the changes that occur in one or other optical phenomenon as the electric field is applied. Measurements of the optical changes lead directly to information on the molecular geometry, flexibility and electrical characteristics. A host of optical phenomena can be used to probe the induced orientation. These include the birefringence (Ref. 2), absorption (Ref. 3), dichroism (Ref. 4), fluorescence (Ref. 5), optical activity (Ref. 6) and scattered light (Ref. 7). In this brief survey birefringence, scattering and fluorescence will be discussed and taken as illustrative procedures.

It is now commonplace to apply the electric field in the form of short duration high voltage pulses. The advent of such pulse technology, accompanied by the appearance of fast optical detectors, makes the methods very fast and versatile. When a burst of electric field is applied to the solution, changes in the recorded optical response are transient in nature. They may be considered as consisting of three temporal regions. Firstly, the initiation of the pulse is accompanied by the coupling of the electric field with the inherent electrical anisotropy of the molecules. The resulting molecular orientation or deformation requires a finite time and hence the observed optical phenomenon builds up in a gradual manner. Secondly, if the electric field is maintained, an equilibrium statistical orientation of the molecules and their segments results and the optical phenomenon reaches a constant value. Finally, the pulse terminates and the molecules revert to their original random array with a gradual return of the optical property to its pre-field value. In general we may characterise the change, ΔA, in any optical property, A, in terms of an orientation distribution function, Φ. Under the equilibrium condition, ΔA is generally proportional to Φ. For a monodisperse solution the decay of the phenomena, after pulse termination, can be approximated by the equation (Ref. 8)

$$\Delta A = \Sigma_i (\Delta A_i)_o \exp - \frac{t}{\tau_i} \qquad (1)$$

Here τ_i are characteristic relaxation times. They may arise from the rotational relaxation of many components of a polydisperse solution of rigid molecules, or the freely relaxing modes of motion of a flexible system. In either case, $(\Delta A)_o$ indicates the field induced change in the optical effect for the relaxing species at the commencement of the decay for which t = 0. Detection and measurement of τ_i can thus be used to indicate either the modes of motion of flexible molecules or the polydisperse nature of a heterogeneous solution.

The orientation function Φ, depends upon the magnitude of the applied field, E. For extremely high limiting fields complete molecular orientation results and $\Phi \rightarrow 1$. At low

fields the electric field couples with any permanent dipole moment, μ, or the anisotropy $\Delta\alpha$ in the electrical polarisability α of the molecules. For rigid molecules under low fields then (Ref. 9)

$$\Phi = \left\{ \frac{\mu_3^2}{(1+9\omega^2\tau^2)\,k^2T^2} + \frac{(\alpha_3 - \alpha_1)}{kT} \right\} E^2/_{15} \qquad (2)$$

In this equation cylindrical molecular symmetry is assumed and the subscripts 3 and 1 indicate the major and a transverse molecular axes respectively. Should a burst of alternating current field be applied, ω represents its angular frequency whilst k and T indicate the Boltzmann constant and the absolute temperature respectively. From equation 2, one sees that by measuring changes ΔA under varying conditions of field strength E, one can evaluate the term in the brace directly. Variation of the frequency of the field provides a means of isolating the permanent and induced dipolar contributions. Rather than measuring and plotting a complete frequency dispersion curve the required data can be established from two electro-optic transient responses. A D.C. field pulse excites both μ and $\Delta\alpha$ contributions. A burst of high frequency A.C. field, of the same r.m.s. field amplitude and pulse duration as the D.C. pulse, but of such a high frequency that the first term in the brace of equation 2 becomes negligible, excites only the $\Delta\alpha$ contribution. This is illustrated in Fig. 1. Analysis of the amplitudes of the two corresponding electro-optical transients enables μ and $\Delta\alpha$ to be isolated.

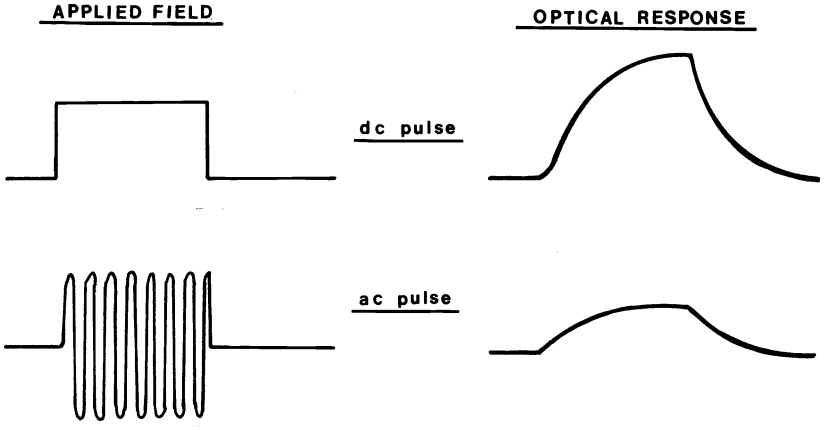

Fig. 1 Hypothetical electro-optical transient responses to D.C. and sinusoidal field pulses. Permanent and induced dipolar mechanisms contribute to the former whilst only induced moments influence the latter.

Thus, electro-optical methods lead to the ready evaluation of τ, μ and $\Delta\alpha$ in addition to information related directly to the structural origins of the optical phenomena themselves. The high sensitivity of τ upon particle dimension has proven to be a good indicator of sample polydispersity, size and conformation change (Ref. 4). The permanent dipole moment has occasionally been used for molecular structure evaluation (Ref. 10). The polarisability is proving of much current interest (Ref. 11). In the case of aqueous and ionic media the molecular-solvent interface gives rise to a strong interfacial polarisability which is measured directly in $\Delta\alpha$. In such cases $\Delta\alpha$ appears to be extremely sensitive to molecular attachment and thus can be used to show aggregation and association phenomena (Ref. 12).

In the interests of brevity this survey is limited to birefringence, scattering and fluorescence phenomena alone as illustrative of the general methods.

ELECTRIC BIREFRINGENCE

Electric birefringence, or the Kerr effect, is the oldest and best established electro-optical method. It has its origins in molecular anisotropy of refractive index or optical polarisability. A birefringent medium can be readily detected by placing it between a 'crossed' polariser and analyser pair and detecting any light transmitted through the system. An apparatus suitable for studying dilute polymer solutions is shown in Fig. 2. It consists of the following. Light from a well collimated source, such as a laser, is sent through a high quality polariser and impinges upon a cell containing the sample. This cell contains a pair of electrodes, generally transversely mounted, either side of the light beam. Such electrodes define the field vector which should be set at 45^o azimuth to the transmission direction of the polariser. When a field is generated between the electrodes and the

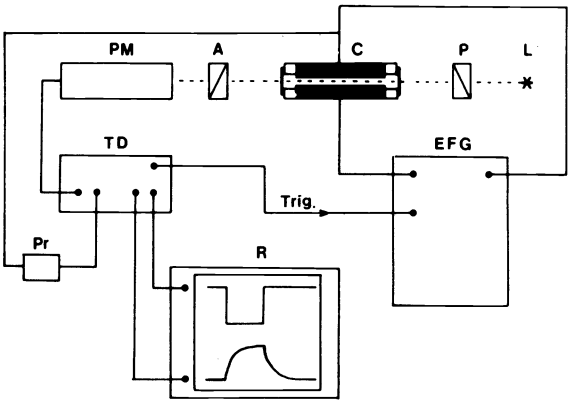

Fig. 2 Schematic Kerr effect apparatus. Components are L - light source; P - polariser; C - sample cell; A - analyser; PM - photomultiplier; TD - transient digitiser; EFG electric field generator; R - recorder; Pr - probe attenuator.

interspace becomes birefringent, elliptically polarised light emerges from the cell. The cell is followed by a second polarising device whose transmission azimuth is at 90° to that of the polariser. Light penetrating such a system has intensity proportional to Δn^2 where Δn defines the birefringence induced (Ref. 13). This light may be conveniently detected using a photomultiplier whose output is amplified and recorded on an oscilloscope or transient digitiser. Special high voltage pulse generators are required to generate voltages of up to a few kV r.m.s. amplitude, with pulse durations ranging in the μs and ms regions. The electrode separation in the cell is typically a few mms, enabling fields of up to 20 kV cm^{-1} to be generated. Additionally for A.C. pulses a variable alternating frequency from zero to the near kHz range is advantageous. Experiments are generally conducted in single-shot mode, although greater sensitivity can be achieved with multiple sequential pulse application together with signal averaging of the responses in cases where the signal is small and the applied field does not interfere with molecular behaviour.

The induced birefringence Δn is defined as the difference in the refractive indices of the medium parallel ($n_{\parallel}$) and perpendicular ($n_{\perp}$) to the field direction. For a solution of volume concentration c and average refractive index n, under equilibrium conditions of orientation, then (Ref. 9),

$$\Delta n = \Delta n_o = \frac{2\pi c}{n} \cdot (g_3 - g_1)\, \Phi \qquad (3)$$

where g_i are the optical polarisabilities along the relevant molecular axes. We restrict ourselves here to the case of rigidly rotating molecules in order to illustrate principles. More complicated equations for flexible systems are given elsewhere (Ref. 14). By measuring Δn_o under high and low field strengths where $\Phi = 1$ and $0 < \Phi < 1$ respectively, $(g_3 - g_1)$, μ and $\Delta\alpha$ are evaluated. Using fast-recording photomultipliers and oscilloscopes, the rapid transient changes in the optical phenomena can be measured and the relaxation time, τ, evaluated from the decay (equation 1). This is conveniently realised by plotting a semi-logarithmic curve of the birefringence amplitude Δn at times t during the decay, in the form of $\ln(\frac{\Delta n}{\Delta n_o})$ vs. t. Curvature in such a plot indicates polydispersity in the sample. The initial slope of the semi-log plot provides a convenient average for τ. Alternatively τ can be treated as a time constant and an average $\bar{\tau}$ obtained from that time t at which the transient decay has fallen to 0.37 of its maximum amplitude. Equations exist in the literature for the analysis of τ in terms of the dimensions of thin rods (Ref. 15), discs (Ref. 16), ellipsoids (Ref. 16) and freely flexible coils (Ref. 17).

A host of systems have been studied by electric birefringence. The majority of studies have been to determine the geometry of rigid and semi-rigid molecules. It has been common to interpret data for flexible systems in terms of the worm-like chain concept and the weakly bending rod model. Equations exist for relaxation time interpretation in terms of these models (Ref. 18). Typical of these studies was the work reported for aqueous solutions of cellulose derivatives (Ref. 19). The following data on a sodium carboxymethyl cellulose sample illustrate the method. Samples of molecular weight (M) from 3 to 25 x 10^4 were studied under field strengths of up to 7 kV amplitude. Pulses of 40 to 200 μs duration were used. Fig. 3 shows the tracing of a typical transient for a sample of M = 30,000. The transient nature of the response is evident as is the fast relaxation time. Before interpreting data according to equation 2 it is usual to verify that at low field strengths the

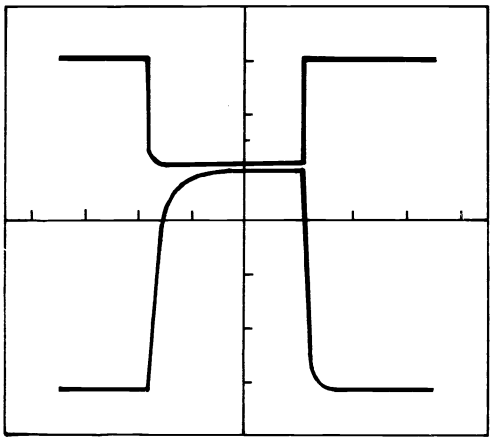

Fig. 3 Birefringence transient for sodium carboxymethyl cellulose in water (lower trace); c = 0.2 mg.ml^{-1}. Upper frame shows the applied field of 145 μs duration and 8.4 kV cm^{-1} amplitude. Time runs from left to right. (Data from Ref. 19).

true Kerr theoretical region in which $\Delta n \propto E^2$ was upheld. In Fig. 4 the dependence of the birefringence on E^2 was evident for low E. This Fig. also showed the conditions for which $\Phi \rightarrow 1$, as at higher field strengths where Δn became independent of E. For this particular system there was no permanent dipole moment and all the birefringence had its origin in

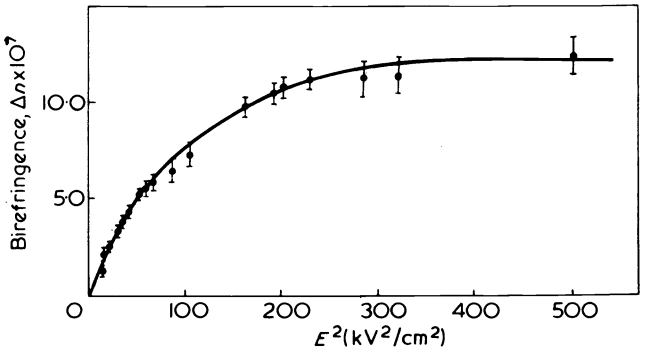

Fig. 4 Variation of induced birefringence with field strength for sodium carboxymethyl cellulose; c = 0.2 mg.ml^{-1} and M = 3 x 10^4. (Data from Ref. 19).

electrical polarisability phenomena. Relaxation times for each polymer sample were obtained from the decay of the birefringence and were analysed in terms of a rigid rod, a weakly bending rod and the worm-like chain. The increasing flexibility of the molecule with increasing molecular weight can be seen in Fig. 5 where the equivalent rod length for a rigid rod has been plotted as a function of M. This flexibility was also exhibited in the variation of the polarisability, again calculated on the assumption of a rigid rod molecule with increasing molecular weight. Departure from the rigid rod approximation occurred increasingly for $M > 8 \times 10^4$. From the high field data with $\Phi \rightarrow 1$ the optical anisotropy $(g_3 - g_1)$ was evaluated. When corrected for the extended length of the polymer, the value of the optical anisotropy per unit polymer extended length of $Lt_{L \rightarrow o}\{(g_3 - g_1)/L\} = 3.7 \times 10^{-24}$ Fm was obtained. Apart from the evaluation of such parameters one should appreciate the extreme rapidity with which τ and hence the polymer size parameters could be evaluated.

A second example, which indicated potential development of the electric birefringence method, is provided by recent studies on aqueous solutions of proteoglycan. This polysaccharide is a major component of cartilage tissue where it readily aggregates with hyaluronic acid and collagen. Extensive research is currently being undertaken to determine the nature of such interaction both in dilute solution and in the cartilage matrix. Cartilage proteoglycans have a complex composition (Ref. 20) (Fig. 6). They consist of a central protein core approximately 300 nm long to which side chains of chondroitin-4-sulphate and keratan sulphate

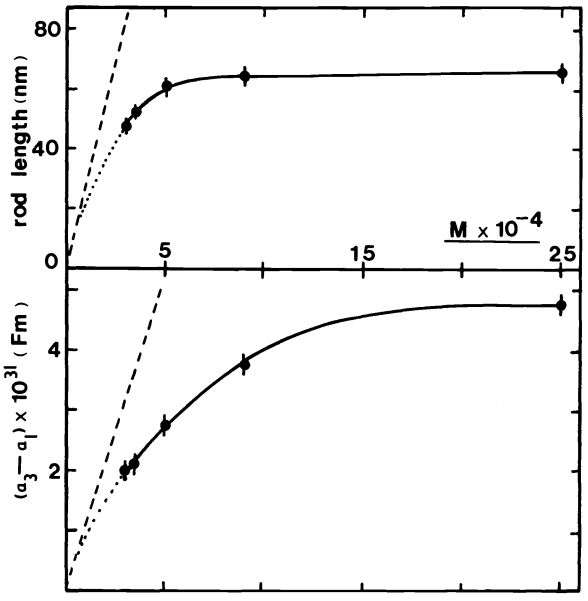

Fig. 5 Variation of equivalent rigid rod length and the excess molecular polarisability with molecular weight for sodium carboxymethyl cellulose. Broken lines indicate true rigid rod behaviour. (Data from Ref. 19).

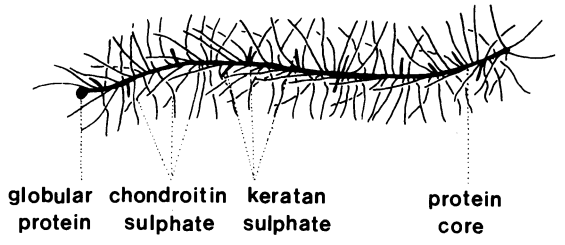

Fig. 6 Diagrammatic representation of the proteoglycan structure

are radially attached. The chondroitin sulphate chains are about 40 nm long and are the predominant side member. Proteoglycan terminates in a globular protein region. Recent electric birefringence studies on proteoglycan solutions have shown the existence of multi-component transient birefringence trace responses (Ref. 22). A typical set of data is shown in Fig. 7, this series of responses having been excited by electric fields of different amplitudes. Three transient components can be detected both by the sign and amplitude of the birefringence and by the relaxation times involved. They are revealed by harnessing a useful property of pulsed fields, namely that one can vary both the amplitude of the field and the duration for which it is applied. Generally larger molecules involve larger dipole moments and need smaller amplitude fields to orientate them. However larger molecules orientate in a viscous medium at a slower rate than their smaller counterparts. Hence by controlling either or both the duration and the amplitude of the field, one can selectively excite each of a series of relaxing phenomena contributing to the ultimate birefringence. The data for proteoglycan have been obtained by varying the field strength alone. They indicate three relaxing components within the molecule. The slowest has been shown to be compatible with the existence in solution of end-to-end dimers (Ref. 21) which orientate with a relaxation time $\tau_1 \triangleq 3$ ms. An intermediate time species corresponds to the deformation and orientation of the individual proteoglycan molecules with $\tau_2 = 400$ to 800 μs. Much larger fields are required to excite the third and fastest component with $\tau_3 \triangleq 2$ μs which has been shown to originate from the flexing of the chondroitin sulphate side chains on the proteoglycan chain (Ref. 22). These experiments are currently being extended both to study the nature of proteoglycan interactions and to develop a method of electric birefringence 'spectroscopy' for the isolation and characterisation of individual components within a multi-component molecular process.

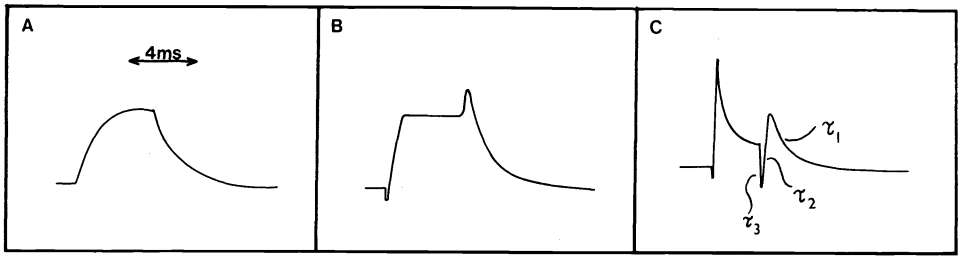

Fig. 7 Complex birefringence transients for proteoglycan solutions. The increasing field strength from (A) to (C) excites faster relaxing species. (A) 200 V cm^{-1}; (B) 680 V cm^{-1}; (C) 2.4 kV cm^{-1}. Numerals indicate the three species with $\tau_1 > \tau_2 > \tau_3$. (Data from Ref. 21).

The simplicity of the apparatus and its manipulation has endeared electric birefringence to an increasing number of polymer scientists. It is the most sensitive of current electro-optical methods, predominantly owing to the fact that the birefringence is induced about a null or zero level. This has the disadvantage in that no additional information is obtained from pre-field measurements. The following methods, though of reduced sensitivity, do offer such additional information.

ELECTRIC FIELD LIGHT SCATTERING

Measurement of the angular dependence of the time averaged scattered intensity from polymer solutions has become a standard procedure for obtaining molecular weight and the radius of gyration of polymer molecules whose major dimension is of the order of the wavelength of light, λ. Intramolecular interference between wavelets scattered from different molecular regions gives rise to an angular dependence of the scattered intensity, I, which is usually analysed in terms of a Zimm plot (Ref. 23). The procedure has been extensively reviewed (Ref. 24,25). Such intermolecular interference, however, is strongly dependent on molecular orientation. Hence alignment of a solute species gives rise to significant changes in the interference pattern and hence in the scattered intensity at various angles θ. Measurement of such changes leads to the evaluation of μ, $\Delta\alpha$ and τ. Analysis of the scattered intensity changes is theoretically more complicated than the birefringence described above. Theories have been developed for rigid and flexible molecules. For rigid molecules at low degrees of orientation the equation (Ref. 7,26)

$$\frac{\Delta I}{I} = (1 - 3\cos^2\Omega) \cdot Q \quad \Phi \tag{4}$$

holds where Q is a parameter independent of the orientational properties of the molecule, but depends upon the particle size, shape and θ. It can be evaluated from data prior to the application of the electric field. The angle, Ω , defines the electric field direction and is in fact the angle between the field direction and the $\bar{s}$ vector. The scattering vector ($\bar{s}$) is formed between unit vectors in the forward and observed directions respectively. Rigid molecules are characterised by the presence of the factor $(1 - 3\cos^2\Omega)$. From equation 4, measurements of ΔI lead to Φ directly. As in the case of other electro-optical phenomena, μ and $\Delta\alpha$ can be isolated from Φ through the frequency dependence of the contributions, provided data are recorded in that region where equation 4 applies, namely where $\Delta I \propto E^2$.

For freely flexible molecules characterised by bonds with the axially directed dipole moment μ_o, the scattered intensity is given by the following equations (Ref. 7) for those specific cases where $\Omega = 0^o$ or 90^o. With $\Omega = 0$,

$$\frac{\Delta I}{I} = \frac{N^2 \mu_o^2}{3 P_o(\theta)} \cdot \left\{ \frac{h a \sin \theta/2}{3} \right\}^2 \left(\frac{E}{kT}\right)^2 \tag{5a}$$

and with $\Omega = 90$,

$$\frac{\Delta I}{I} = \frac{2N \mu_o^2}{15 P_o(\theta)} \left\{ \frac{h a \sin \theta/2}{3} \right\}^2 \cdot \left(\frac{E}{kT}\right)^2 \tag{5b}$$

where $h = \left(\frac{2\pi}{\lambda}\right)$ and the chains are assumed to consist of N segments of identical length (a) with $a < \lambda$. Also $P_o(\theta)$ is the particle scattering factor for random coils, namely

$$P_o(\theta) = \frac{2}{Z^2} \cdot \left[\exp(-Z) - (1-Z)\right] \quad (6)$$

with

$$Z = 0.66\, h^2 \sin^2(\theta/2) \cdot N a^2 \quad (7)$$

The more complicated case, where μ_o is not directed along the segmental element, has been summarised elsewhere (Ref. 27). From these equations one notes two factors. Firstly the changes no longer depend upon Ω according to the factor $(1 - 3\cos^2\Omega)$ as in the case of rigid molecules. Secondly the scattering changes are much larger for $\Omega = 0$ than 90, as is seen from the dependence on N^2 rather than N. In reality, ΔI for $\Omega = 90$ is negligible. One can thus use equation 5a for the evaluation of μ_o for polar chains. As before, relaxation times can be evaluated by studying the decay of the scattered intensity following the termination of any applied pulse (Ref. 28). This parameter is especially interesting when compared with the radius of gyration (S) obtained from the pre-field scattering experiments. Each of these parameters depends to a different power on the basic size parameter. For example $S \propto L$ for a rod of length L, but $\tau \propto L^3$. Hence one can estimate molecular geometry from measurements of τ and S alone, for only one geometry will satisfy both experimental parameters. This has been used in the analysis of the geometry of complicated clay mineral aggregates (Ref. 29) and in one polymer conformation study (Ref. 30).

Conventional scattering photometers can be readily adapted for electric field measurements. The requirements are as follows. Firstly suitable electrodes must be incorporated in the cell so that the field can be applied. Most conveniently a pair of horizontal electrodes, spaced either side of the incident light beam, allow the electric field to be applied. Cells with vertically placed electrodes, although less convenient to use experimentally, are of value in indicating molecular flexibility (see below). Secondly, the light source must be run from a stabilised D.C. electrical power supply. Alternating variations in the lamp output interfere with the light detection. Thirdly, provision must be made for recording transient changes in the scattered intensity. Conventional instruments use meter readings and smoothed long-time outputs. These are not acceptable. Finally, the auxiliary apparatus for pulse generation is also required. Details of these and other modifications have been given elsewhere (Ref. 26).

Experimental data for a solution of nitrocellulose in acetone provide illustrative data (Ref. 31). The nitrocellulose sample had some 12% nitrogen content corresponding to an average degree of substitution of 4.6 nitro groups per cellobiose unit. A typical Zimm plot was obtained from which $\bar{M}_w = 4.6 \times 10^5$ and $(\overline{S^2})_Z^{\frac{1}{2}} = 101$ nm were determined. Electro-optic data were recorded for both $\Omega = 0^o$ and $\Omega = 90^o$ using the cell described below (Frame I of Fig. 10). The field dependence of the scattered intensity changes are shown in Fig. 8 for fields up to 2.3 kV m^{-1}. Data were also recorded over a range of alternating field frequencies up to 15 kHz. The frequency dependence of the scattered intensity changes is shown in Fig. 9 alongside theoretical dispersion curves for theoretical values of τ. The rigidity parameter R discussed below was of the order of -1.5. A freely rotating completely rigid system would be characterised by R = -2. Such a small deviation from 2 is not considered to

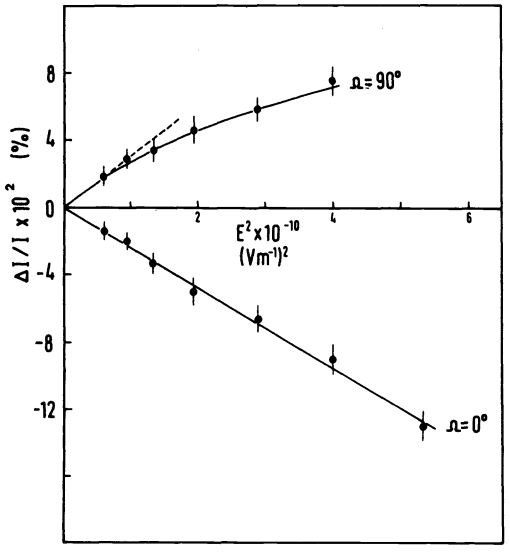

Fig. 8 Field strength dependence for the scattered intensity changes of nitrocellulose in acetone. Data for $\Omega = 90^o$ and 0^o at $\theta = 90^o$ and $\lambda = 436$ nm. (Reproduced from Ref. 31).

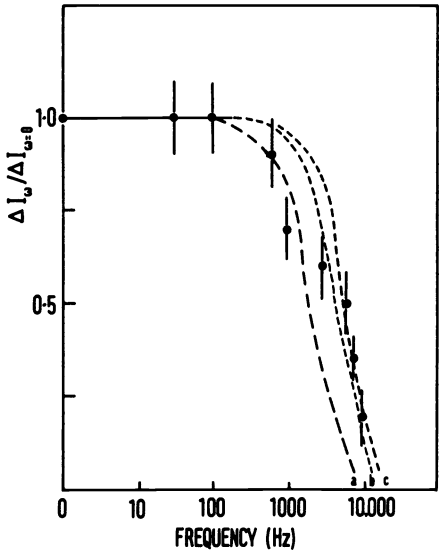

Fig. 9 Frequency dispersion of the scattered intensity change for nitrocellulose. $\theta = \Omega = 90^{o}$, λ = 436 nm, E = 710 V cm^{-1}. Broken lines for Debye dispersions with (a) τ = 50 μs; (b) τ = 36 μs; (c) τ = 29 μs. (Reproduced from Ref. 31).

be significant. Hence, a system of stiff but not completely rigid molecules is indicated. The equations for freely rotating polar flexible chains given above are therefore inappropriate to this system. Assuming the absence of any induced dipole moment, it is convenient to use the equation for rigid rod molecules of length L. In such a case equation 4 can be expressed as

$$\frac{\Delta I}{I} = (1 - 3\cos^2\Omega) \cdot Q \cdot \frac{\mu^2 E^2}{k^2 T^2 \left[1 + (3\omega\tau/2)^2\right]} \qquad (8)$$

where τ is given by the Broersma (Ref. 15) equation. Using the experimental data for τ = 36 μs together with the rod length of 350 nm obtained from the radius of gyration, the dipole moment of the complete molecule was 5.2 x 10^3 Debye. For this molecular weight, the degree of polymerisation was 10^3. Hence a value of the monomer dipole moment μ_o = 5.2 Debye was obtained. This is in close agreement with the value of 6 Debye obtained by dielectric data (Ref. 32) and suggests that nitrocellulose is indeed extremely stiff in this solvent. In conclusion, this study not only indicated the stiffness of the polymer in the solvent but also enabled M, S, μ, μ_o and τ to be evaluated. Few other methods yield such a host of parameters from a single experiment.

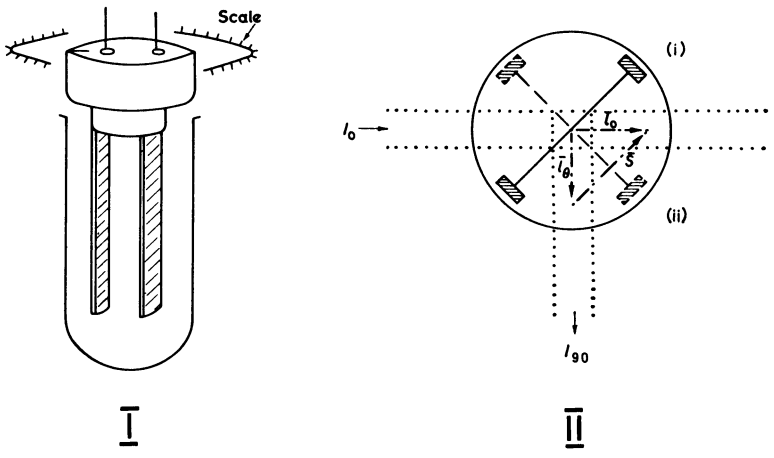

Fig. 10 Light scattering cell with vertical electrodes for increasing the rigidity parameter R. (I) the cell; (II) plan view showing positions (i) and (ii) for electrodes relative to $\bar{s}$ vector.

Use of electric field scattering data to indicate molecular flexibility and/or rigidity has been mentioned above. From equations 5a and 5b one sees that if measurements are recorded of $\Delta I_{\Omega=0}$ and $\Delta I_{\Omega=90}$, then one can define the ratio

$$R = {}^{(\Delta I)}\Omega=0 \,/\, (\Delta I)_{\Omega=90} .$$

For all rigid molecules this ratio has the value -2. A polar freely flexible molecule with axially directed dipole moments is characterised by $R = \frac{-5N}{2}$. Hence relative intensity changes ΔI under conditions of $\Omega = 0^o$ and $\Omega = 90^o$ immediately indicate particle rigidity. A suitable experimental cell has been designed for the rapid determination of R. The cell is shown in frame I of Fig. 10 and its principle of operation given in II. With the electrodes set in position (i) and the scattered intensity measured at $\theta = 90^o$, E is parallel to $\bar{s}$ and $\Omega = 0^o$. Rotation of the electrodes through 90^o to positions (ii) generates the conditions for $\Omega = 90^o$. Hence without having to change the solution or alter the apparatus arrangement one can rapidly obtain a measure of R. This extremely simple procedure is very useful for rapid indication of molecular flexibility. A study on the helical polypeptide poly-L-proline in its form II conformation indicated the existence of freely flexible helical polymer (Ref. 33). Measurements were made with $\Omega = 0^o$ and 90^o with the result that the only measurable changes were detected when $\Omega = 0^o$. This indicated the applicability of equations 5 and the flexibility of the helix, which is assumed to bend back upon itself into an approximately randomly coiled conformation in solution.

The light scattering method is predominantly advantageous for macromolecules of the order of a wavelength of light. This is the condition under which one obtains the most information from the intensity prior to the application of the field and for which one records the greatest intensity changes when the fields are applied. Extremely small changes are obtained for particles less than the wavelength of light whilst those significantly greater than λ invoke the need for the complex Mie scattering theory. Within this limited range and for particles which are polar and of significant stiffness, the method has great potential. As with all electro-optical methods however the method has limited appeal for highly conducting media.

ELECTRO-FLUORESCENCE EFFECTS

Fluorescence is a two-fold optical phenomenon involving both the absorption and subsequent re-emission of light by a molecule. These processes take place along specific directions or transition moments within the structure of an active fluorescent chemical group (fluorophore). Light absorption, and hence ultimate fluorescence, is optimised when the incoming light is polarised parallel to the relevant absorption transition moment. The emitted light is polarised predominantly parallel to the emission transition moment direction. Hence for an incoming light beam of appropriate wavelength and polarised in a given specific direction, the fluorescence can be optimised by orienting all the constituent fluorophores such that their absorption moment is parallel to the polarisation state. Orientation perpendicular to this state minimises the fluorescence. Thus macromolecules which are composed of regularly repeating chemical groups which are fluorophores for given incident light will exhibit changes in their fluorescent properties when aligned from a random state into directional order under the influence of an applied electric field. Alternatively, molecules

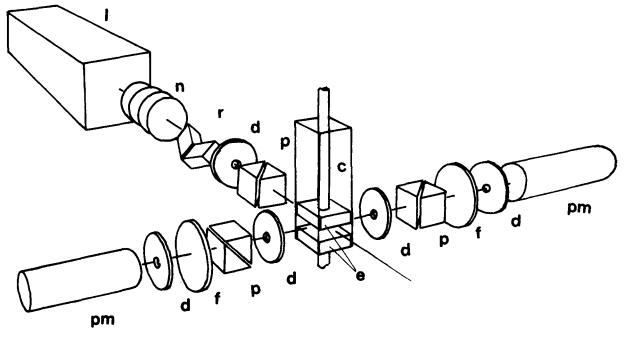

Fig. 11 Apparatus for measurement of electro-fluorescence effects. For component nomenclature see text. Two similar detection limbs record the horizontally and vertically polarised emitted light for a linearly polarised incident beam. (Reproduced from Ref. 34).

which are not fluorescent for a given instant radiation may become so when tagged with certain active fluorescent dye molecules. Ordered attachment to the macromolecule which can then itself be aligned in an electric field will result in changes in the observed components of polarisation of the fluorescence for the solution as a whole. Because of the high sensitivity of fluorescent phenomena one has an electro-optical method of increasing importance which has great potential in indicating the geometry of chemical groups within a macromolecular structure, or the geometry of attachment of fluorescent ligands and dyes when bound to suitable macromolecules. The principal features of the apparatus are shown in Fig. 11. The optical components are designated as follows. Light from a suitable laser L, is suitably attenuated through neutral density filters n, passed through a pair of Fresnel rhombs r, a diaphragm d, and a polariser p. Hence linearly polarised light of selectable azimuth is incident upon the sample cell c, which holds the sample between a pair of electrodes, designated e. Two optical limbs detect the emitted light polarised in perpendicular directions. Each consists of diaphragms d, an analysing polariser p, an optical cut-off filter f, and a photomultiplier pm. The measurements consist in recording four polarised components of fluorescence. Two polarised incident states are accessible and are designated V and H for vertically and horizontally polarised light respectively. One detects the horizontal and vertical polarised emitted beams. In the field, changes in each of these components are recorded and are designated ΔV_V, ΔV_H, ΔH_V and ΔH_H respectively, where subscripts indicate the emitted light conditions. From measurements of each of these components, the directional binding geometry of the fluorophores relative to the macromolecular axes can be discretely determined.

Data have been recorded for an aqueous sample of polymethacrylic acid tagged with acridine orange. The applied field was of 5.6 $kV.cm^{-1}$ amplitude. Using an argon-ion laser, the exciting wavelength was 488 nm and detection was for wavelengths in excess of 515 nm. The responses are shown in Fig. 12. The approximate geometry of binding could be appreciated in a quantitative manner from this figure directly. From other electro-optical measurements it was known that in an electric field the polymer molecules tended to align with their long axes parallel to the field direction owing to the existence of an induced dipole moment.

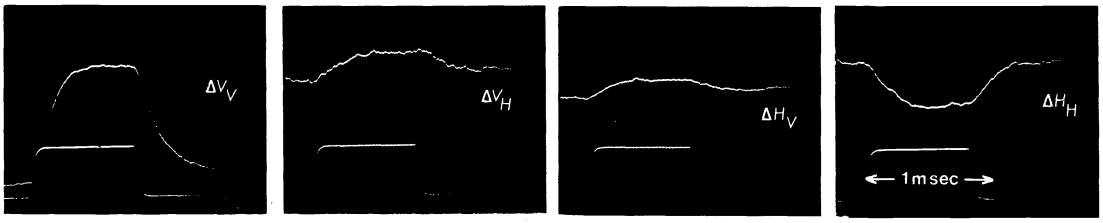

Fig. 12 Transient changes in the polarised components of fluorescence for atactic polymethacrylic acid/acridine orange complex in water. $c = 4.5 \times 10^{-5} g.ml^{-1}$; $E = 5.6\ kV.cm^{-1}$; $\lambda_{in} = 488$ nm; $\lambda_{out} > 515$ nm. The field pulse is the lower trace in each case. Time runs from left to right. (Data from Ref. 35).

With the present geometry the field vector was vertical. Consider the first two frames of Fig. 12. Vertically polarised light was incident on a system which oriented towards the vertical in the electric field. Both polarised components of the emergent fluorescence increased in the field and were thus enhanced by such an orientation of the macromolecule. The fluorophores were thus appended to the polymer with their absorption moment predominantly parallel to the polymer backbone. Furthermore the component ΔV_V was greater than the change ΔV_H, signifying that more light was emitted polarised in the vertical direction than the horizontal. Hence the emission moment was also predominantly associated with the polymethacrylic acid backbone. Acridine orange is a planar ring compound in which both absorption and emission transition moments lie predominantly in the plane of the rings. Hence Fig. 12 is consistent with the acridine orange molecules aligning with their major axes predominantly parallel to the backbone of the polymer. A similar reasoning was obtained by considering the components observed when horizontally polarised light was incident. In this particular study the polymethacrylic acid was atactic and of 7.8×10^5 molecular weight.

An interesting comparison is afforded by the data in Fig. 13. These were recorded for a solution of DNA to which neutral red dye had been attached (Ref. 36). The DNA had a molecular weight of 6×10^6 and existed in solution at a concentration of $4.5 \times 10^{-5} g.ml^{-1}$. The bound dye corresponded to a phosphorus to dye ratio of some 250. Electric fields of 2.7 kV cm^{-1} were applied for 0.8 ms duration. The same apparatus geometry was used as in the experiments for the polymethacrylic acid/acridine orange system. Immediate inspection shows that a completely different set of transient responses was obtained with the DNA system. Considering the polarised components of fluorescence with vertically incident light and applying the reasoning of the aforementioned section, one sees that the neutral red was bound to the DNA predominantly perpendicular to the major backbone axis of the double helix.

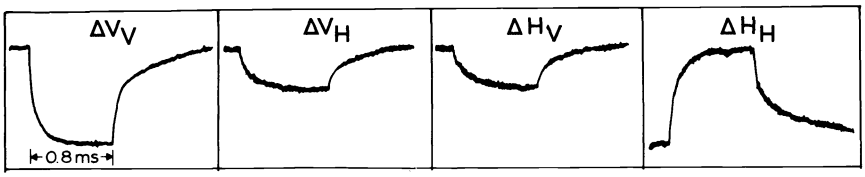

Fig. 13 Polarised components of fluorescence changes for DNA/neutral red complex. $c = 4.5 \times 10^{-5} g.ml^{-1}$; $E = 2.7$ kV cm^{-1}; $\lambda_{in} = 488$ nm; $\lambda_{out} > 515$ nm. Time runs left to right. (Reproduced from Ref. 36).

Such association is common for many dyes and is consistent with the well known model of dye intercalation in the DNA helix in which the planar ring dye compounds bind parallel to the base pairs of the helix.

Current efforts are being made to develop the theory of the electro-fluorescence method. Equations have been given for rigid molecules orienting in an electric field (Ref. 37). From these one can determine precisely the directions of the absorption and emission transition moments for all positions intermediate between parallel and perpendicular binding for truly rigid molecular segments. Furthermore, from measurements of the polarised components of fluorescence prior to the application of the field one can also evaluate the efficiency of binding of the dye. Finally it is emphasised that both the dipole moments and electrical polarisabilities of the molecules can be evaluated from the data, as can the relaxation time and hence the molecular sizes from the rates of decay of the transient changes.

Acknowledgement - Permission from publishers to reproduce figures in full or part is gratefully acknowledged. These include I.P.C. Press Ltd. for Figs. 3, 4, 5, 12 and 13; Pergamon Press for Figs. 8 and 9; Plenum Press for Fig. 7 and The Mineralogical Society for Fig. 11.

REFERENCES

1. D.W. van Krevelen, Properties of Polymers, Chapter 11, Elsevier, Amsterdam (1972).
2. C.T. O'Konski, Encyclopedia of Polymer Sci. and Technol. 9, 551-590 (1969).
3. K. Yoshioka and H. Watanabe, Physical Principles and Techniques of Protein Chemistry, p. 335-367, (Ed. S. Leach) Academic Press, New York (1969).
4. E. Fredericq and C. Houssier, Electric Dichroism and Electric Birefringence, Clarendon Press, London (1973).
5. G. Weber, J. Chem. Phys. 43, 521-524 (1965).
6. I. Tinoco, J. Amer. Chem. Soc. 81, 1540-1544 (1959).
7. C. Wippler, J. Chim. Phys. 53, 316-327 (1956).
8. H. Benoit, Ann. Phys. (Paris) 6, 561-609 (1951).
9. A. Peterlin and H.A. Stuart, Handbuch und Jahrbuch der Chemischen Physik 8 (Sec 1B), Becker & Erler, Leipzig (1943).
10. B.R. Jennings and B.L. Brown, Europ. Polymer J. 7, 805-826 (1971).
11. E. Selegny (Ed.), Polyelectrolytes, Reidel, Dordrecht, Holland (1974).
12. S.P. Stoylov and I. Petkanchin, J. Coll. Int. Sci. 40, 159-163 (1972).
13. J. Badoz, J. Phys. Radium (Paris) 17, Suppl. 11, 143A-149A (1956).
14. D.A. Dows, J. Chem Phys. 41, 2656-2660 (1964).
15. J. Broersma, J. Chem. Phys. 32, 1626-1631 (1960).
16. F. Perrin, J. Phys. Radium (Paris) 5, 497-510 (1934).
17. W.H. Stockmayer and M. Baur, J. Amer. Chem Soc. 86, 3485-3489 (1964).
18. J.E. Hearst, J. Chem. Phys. 38, 1062-1065 (1963).
19. A.R. Foweraker and B.R. Jennings, Polymer 16, 720-724 (1975).
20. H. Muir and T.E. Hardingham, MTP International Review of Science, series I, 5 (1975).
21. E.Y. Hawkins, M. Isles, A.R. Foweraker, B.R. Jennings, T. Hardingham and H. Muir, Electro-optics and Dielectrics of Macromolecules and Colloids, p. 211-218, (Ed. B.R. Jennings) Plenum, New York (1979).
22. K. Kikuchi, B.R. Jennings and M. Isles, Int. J. Biol. Macromols. 3, 53-54 (1981).
23. B.H. Zimm, J. Chem. Phys. 16, 1099-1116 (1948).
24. K.A. Stacey, Light Scattering in Physical Chemistry, Butterworths, London (1956).
25. M.B. Huglin (Ed.), Light Scattering from Polymer Solutions, Academic Press, New York (1972).
26. B.R. Jennings, Chapter 13 in Ref. 25.
27. M.L. Wallach and H. Benoit, J. Polymer Sci., (A2) 4, 491-500 (1966).
28. S.P. Stoylov and S. Sokerov, J. Coll. Int. Sci. 24, 235-240 (1967).
29. J.F. Schweitzer and B.R. Jennings, J. Coll. Int. Sci. 37, 443-457 (1971).
30. H. Plummer and B.R. Jennings, Europ. Polymer J. 6, 171-180 (1970).
31. B.R. Jennings and J.F. Schweitzer, Europ. Polymer J. 10, 459-464 (1974).

32. S.K.K. Jatkar and D.S. Sastry, J. Univ. Poona Sci. Technol. 4, 55-63 (1953).
33. B.R. Jennings, Brit. Polymer J. 1, 70-75 (1969).
34. P.J. Ridler and B.R. Jennings, Clay Minerals 15, 121-133 (1980).
35. P.J. Ridler and B.R. Jennings, Polymer 19, 627-631 (1978).
36. P.J. Ridler and B.R. Jennings, Int. J. Biol. Macromols. 2, 313-317 (1980).
37. G. Weil and J. Sturm, Biopolymers 14, 2537-2553 (1975).